Noname manuscript No.
(will be inserted by the editor)

Flux-profile relationship for dust concentration in the stratified atmospheric surface layer

L. S. Freire · M. Chamecki · J. A. Gillies

Received: DD Month YEAR / Accepted: DD Month YEAR

Abstract Flux-profile relationships are usually obtained under the assumption that the mean field of interest is in equilibrium with the associated surface fluxes. In this study, the existence of an equilibrium state for dust concentration in the atmospheric surface layer above sources and sinks is evaluated using Large-Eddy Simulation. Results showed that for steady-state turbulence and negligible horizontal advection, an equilibrium mean vertical profile of dust concentration is reached after one boundary layer eddy turnover time. This is true for cases over source or sink, under different atmospheric stabilities, and for particles with negligible or significant settling velocity. A new model relating the net surface flux to the vertical concentration profile that accounts for both atmospheric stability and particle settling velocity is proposed. The model compares well with the simulation results for all particle sizes and atmospheric stability conditions evaluated, and it can be used to estimate the concentration profile based on the surface flux, and also to estimate the surface flux by fitting the vertical concentration profile. The resulting equation can be considered as an extension of Monin-Obukhov similarity theory to concentration of settling particles, such as mineral dust, sea-salt, pollen and other suspended aerosols.

Keywords Dust deposition · Dust flux · Equilibrium profiles · Suspended heavy particles

L. S. Freire
Dept of Meteorology, The Pennsylvania State University, University Park, PA 16802, USA
E-mail: freirelivia@psu.edu

M. Chamecki
Dept of Meteorology, The Pennsylvania State University, University Park, PA 16802, USA
E-mail: chamecki@psu.edu

J. A. Gillies
Division of Atmospheric Sciences, Desert Research Institute, Reno, NV 89512, USA
E-mail: jackg@dri.edu

1 Introduction

Dust ejected from soil surfaces by the wind is a major contributor to the aerosol concentration in the atmosphere, impacting climate and air quality from local to global scales. Soil dust can affect the climate directly by changing the net radiation, and indirectly by interfering with cloud formation and precipitation (Zhao et al., 2003). It can also serve as a catalytic reactor for gases in the atmosphere, modifying bio-geochemical processes in air and oceans (Ginoux et al., 2001). Dust is composed of solid inorganic particles of diameter $< 62.5\,\mu$m, usually derived from sediment formed by weathering and erosion of rocks (Kok et al., 2012). Once dust particles are lifted from the surface, they are mainly transported in suspension. Consequently, the dust concentration in the atmosphere is strongly influenced by the particle gravitational settling and atmospheric turbulence (Tsoar and Pye, 1987). While gravitational settling limits the lifetime of dust in the air reducing transport distances (only particles smaller than $20\,\mu$m of diameter can remain suspended long enough to substantially affect weather and climate (Kok et al., 2012)), more vigorous turbulence produced by buoyancy can enhance this lifetime. Similarly, the deposition velocity of suspended particles can also be modulated by the effects of atmospheric stability on turbulence intensities. Therefore a theoretical framework that considers the effects of gravitational settling and atmospheric stability on dust fluxes is highly desirable.

The simplest approach for the development of such a theory is to seek steady-state relations between surface fluxes and mean vertical concentration profiles over very large dust sources or sinks (hereafter "profile" will be used to refer to "vertical profile"). If available, this relation can be used to estimate atmospheric dust loads from surface fluxes as well as to estimate surface fluxes from observed mean concentrations. The latter is also relevant in the representation of surface fluxes of dust in numerical simulations. Turbulence resolving numerical simulations of the ABL focusing on particle dispersion usually parameterize the surface flux (both the source and the deposition) as a function of the resolved concentration at a reference height (Chamecki et al. 2009, Chamecki and Meneveau 2011, Pan et al. 2013). In this application, a simple yet effective model that captures the effects of particle size and atmospheric stability on the flux-concentration relation is needed. During long-distance transport events relevant for regional air quality considerations and climate processes, dust particles $> 5\,\mu$m are predominantly removed from the atmosphere by dry deposition (Kok et al., 2012). Therefore, another application is the parameterization of dry deposition velocity in regional and global climate models (Zender et al. 2003, Gong et al. 2003, Ginoux et al. 2001, Nho-Kim et al. 2004).

The first theoretical equilibrium profile of mean particle concentration was proposed by Prandtl (1952), and it was derived based on the steady-state mean conservation equation for "heavy" particle concentration under the assumptions of zero surface net flux and neutral atmospheric stability. Chamberlain (1967) and Kind (1992) extended the model to non-zero surface fluxes. Chamecki et al. (2007) generalized the approach to include the effects of atmospheric stability, presenting comparisons with observed profiles of corn pollen concentration above a cornfield. The main limitation of the model presented by Chamecki et al. (2007) is that in the limit of very small particles (when the gravitational settling is negligible), the equation does not recover the classic result obtained from Monin-Obukhov similarity theory (Monin and Obukhov, 1954) for passive scalars. Thus, a unified framework that accounts for effects of atmospheric stability and is valid across the entire range of particle sizes is still lacking.

Another standing issue is the set of conditions required for the existence of equilibrium solutions. In particular, over very large sources for which mean horizontal advection is negligible, the existence of equilibrium solutions with non-zero net surface fluxes has been questioned (Hoppel et al., 2002). If a zero net flux is required, then Prandtl's model is the only possible solution. However, an idealized model study by Xiao and Taylor (2002) has shown that equilibrium solutions with non-zero net flux exist for small particles. Resolving this issue is extremely important, because if no equilibrium profile exists with a non-zero surface net flux, then these simple equilibrium models cannot be used to retrieve surface fluxes from mean concentration measurements nor to parameterize deposition fluxes in numerical models.

In this context, the objectives of the present study are the following: (i) to investigate the applicability of equilibrium solutions for dust concentration profiles over large sources and sinks; (ii) to develop a new analytical equilibrium model relating surface flux and profiles of mean dust concentration that accounts for effects of particle size and atmospheric stability with a non-zero net surface flux; and (iii) to assess the accuracy of different equilibrium solutions in retrieving surface fluxes from mean concentration profiles. Simulations of the dust transport in the ABL were performed using the Large-Eddy Simulation (LES) technique for neutral, unstable and stable thermal stabilities, with different particle sizes, with emission and deposition surface fluxes. Simulation results were used to evaluate the steady-state hypothesis and the performance of the various equilibrium models in reproducing mean profiles and estimating surface fluxes. Based on the results, the applicability of each equilibrium model is discussed.

The next section presents the description of existing equilibrium models for the mean concentration profile, followed by the derivation of a new model. Section 3 describes the LES simulations performed in the present study. In Section 4, the steady-state hypothesis is evaluated from the simulation data, and the performance of different equilibrium models is assessed. Conclusions are presented in Section 5.

2 Models for the mean concentration dust profile

2.1 Existing models for mean concentration profile

The usual approach to relate flux and mean concentration profiles of dust introduced by Prandtl (1952) is based on the Reynolds-averaged conservation of mass of dust particles (hereafter assumed to be monodisperse). The equation for a horizontally homogeneous flow with no mean vertical velocity is

$$\frac{\partial \overline{C}}{\partial t} = w_s \frac{\partial \overline{C}}{\partial z} - \frac{\partial}{\partial z} \overline{w'c'} + \frac{\partial}{\partial z}\left(D \frac{\partial \overline{C}}{\partial z} \right), \tag{1}$$

where $\overline{C}$ is the mean concentration of particles, $\overline{w'c'}$ is the vertical turbulent flux, z is height, t is time, w_s is the particle settling velocity (assumed to be constant), and D is the diffusivity due to Brownian motion. Note that the assumption of source or sink with a large extent is implicit in the fact that horizontal advection is neglected. Parameterizing the turbulent flux in terms of an eddy diffusivity K_C, neglecting Brownian diffusion, and assuming that the mean concentration is constant in time, vertical integration of Equation (1) yields

$$-K_C \frac{d\overline{C}}{dz} - w_s \overline{C} = \Phi. \tag{2}$$

The first term on the left side of Equation (2) represents the turbulent flux of dust particles and the second term represents the flux due to gravitational settling. The constant of integration Φ represents the net vertical flux of dust (Kind, 1992; Chamecki et al., 2007). For the present problem, the source or sink is located at the ground and Φ can be interpreted as the net surface dust flux. Note that the assumptions leading to Equation (2) imply that the net flux must be constant in time and space.

Different models for the mean concentration profile of particles have been obtained from Equation (2), corresponding to different assumptions for K_C, Φ and w_s. Prandtl (1952) assumed that the transport of particles by turbulent diffusion is balanced by gravitational settling, resulting in a zero net flux (which corresponds to Equation (2) with $\Phi = 0$). Assuming the particle eddy diffusivity to be equal to the momentum diffusivity $K_C = \kappa z u_*$ (κ is von Karman's constant and u_* is the wind friction velocity), integration yields Prandtl's power-law model for the normalized vertical profile

$$\frac{\overline{C}}{\overline{C}_r} = \left(\frac{z}{z_r}\right)^{-w_s/\kappa u_*}, \tag{3}$$

where $\overline{C}_r$ is the mean concentration at a reference height z_r.

As pointed out by Kind (1992), the problem of using Equation (3) is that the net flux Φ is in general not zero. Chamberlain (1967) and Kind (1992) proposed a more general model by integrating Equation (2) with a non-zero constant Φ:

$$\frac{\overline{C}}{\overline{C}_r} = \left(\frac{\Phi}{\overline{C}_r w_s} + 1\right)\left(\frac{z}{z_r}\right)^{-w_s/\kappa u_*} - \left(\frac{\Phi}{\overline{C}_r w_s}\right). \tag{4}$$

In the limit of vanishing settling velocity ($w_s \to 0$), this model (hereafter referred to as Kind's models) tends to the log-law profile obtained from similarity theory for neutral stability conditions (Monin, 1970):

$$\frac{\overline{C}}{\overline{C}_r} = 1 - \frac{\Phi}{\kappa u_* \overline{C}_r} \ln\left(\frac{z}{z_r}\right). \tag{5}$$

The solution (4) also recovers Prandtl's model (3) when the net flux is zero ($\Phi = 0$). Therefore, Kind's model corresponds to a complete representation of $\overline{C}/\overline{C}_r$ for different settling velocities and constant net fluxes.

Models (3)–(5) are valid for neutral stability, and their use is typically justified on the basis that aeolian transport only occurs at high wind speeds, and that neutral stratification is a good approximation under these conditions (Kind, 1992). However, significant transport may occur under unstable conditions (Chamecki et al., 2007; Klose and Shao, 2013). By analogy with Monin-Obukhov (MO) similarity theory, Chamecki et al. (2007) assumed that the dimensionless total vertical flux of particles, composed of turbulent and settling fluxes, is a function of the dimensionless stability parameter $\zeta = z/L$, where $L = -u_*^3\overline{\theta}_s/(\kappa g \overline{w'\theta'}|_s)$ is the Obukhov length ($\overline{\theta}_s$ and $\overline{w'\theta'}|_s$ are the temperature and sensible heat flux at surface, respectively, and g is gravitational acceleration). Therefore, their assumption can be written as

$$\frac{1}{\Phi}\left(\frac{\kappa z u_*}{Sc_t}\frac{\mathrm{d}\overline{C}}{\mathrm{d}z} + w_s\overline{C}\right) = -\phi_c(\zeta). \tag{6}$$

For lack of a better alternative, they used the similarity function for passive scalars given by Kaimal and Finnigan (1994),

$$\phi_c(\zeta) = \begin{cases} (1-16\zeta)^{-1/2}, & \text{if } \zeta < 0 \text{ (unstable)},\\ 1+5\zeta, & \text{if } \zeta > 0 \text{ (stable)},\\ 1, & \text{if } \zeta = 0 \text{ (neutral)}. \end{cases} \tag{7}$$

The solution of Equation (6) is

$$\frac{\overline{C}}{\overline{C}_r} = \left[\frac{\Phi}{\overline{C}_r w_s}\Omega\left(\frac{z_r}{L}\right) + 1\right]\left(\frac{z}{z_r}\right)^{-\eta} - \frac{\Phi}{\overline{C}_r w_s}\Omega\left(\frac{z}{L}\right), \tag{8}$$

where $\eta = w_s Sc_t/(\kappa u_*)$ is the Rouse number and $Sc_t = K_M/K_C$ is the turbulent Schmidt number, which accounts for differences between the eddy diffusivity of particles (K_C) and the eddy viscosity (K_M). The atmospheric stability correction function is calculated via

$$\Omega(\zeta) = \begin{cases} {}_2F_1(\eta, 1/2; 1+\eta; 16\zeta), & \text{if } \zeta < 0 \text{ (unstable)},\\ 1+5\left(\frac{\eta}{\eta+1}\right)\zeta, & \text{if } \zeta > 0 \text{ (stable)},\\ 1, & \text{if } \zeta = 0 \text{ (neutral)}, \end{cases} \tag{9}$$

where ${}_2F_1(\eta, 1/2; 1+\eta; 16\zeta)$ is the Gaussian hypergeometric function (Lebedev, 1972; Chamecki et al., 2007).

Equation (8) is a model for the concentration profile of dust as a function of the particle diameter (through the settling velocity w_s), the net flux Φ, and the atmospheric stability ζ. This model recovers Kind's model (4) with the inclusion of the turbulent Schmidt number Sc_t when the ABL is neutral (note that the limit works for both the stable and the unstable expressions, because in the latter ${}_2F_1 \to 1$ when $\zeta \to 0$). In the limit for very small particles ($w_s \to 0$), the model should recover the expression for MO similarity theory for a passive scalar. However, in this limit we have $\Omega(\zeta) \to 1$ for both the unstable and stable expressions in Equation (9) (note that ${}_2F_1 \to 1$ for $w_s \to 0$). Therefore the effects of atmospheric stability vanish for small particles and the model proposed by Chamecki et al. (2007) tends to Kind's model and not the expressions from MO similarity theory, suggesting that there is a problem with that solution. Note that Equation (6) approaches MO similarity theory for $Sc_t = 1$ and $w_s \to 0$ (i.e. it recovers Equation (10) if one replaces $\Phi = -K_C d\overline{C}/dz$), and the problem arises during the integration leading to (8). Note also that Equation (6) is certainly not the most natural way to include effects of atmospheric stability (as discussed later) and that it cannot be recast in the general form (2).

2.2 A new general solution for mean concentration profile

A new solution to Equation (2) can be obtained by using a more general model for the turbulent diffusivity K_C. Following the standard approach from Monin-Obukhov similarity theory, the effect of atmospheric stability can be incorporated in the parameterization of the turbulent diffusivity (Kaimal and Finnigan, 1994; Shao, 2000)

$$K_C(\zeta) = \frac{\kappa z u_*}{\phi_c(\zeta)}. \tag{10}$$

In addition, the trajectory-crossing effect (Csanady, 1963) on the turbulent diffusivity has to be taken into account. This is done by replacing K_C by $K_{C,p} = \alpha_{tc} K_C$, where α_{tc} represents a reduction in the turbulent diffusivity due to the trajectory-crossing effect. Following the model proposed by Csanady (1963), the correction for the vertical turbulent diffusivity is given by

$$\alpha_{tc} = \left(1 + \beta^2 \frac{w_s^2}{\sigma_w^2}\right)^{-1/2} = \left(1 + \beta^2 \frac{w_s^2}{u_*^2 \phi_w^2}\right)^{-1/2}. \tag{11}$$

Here β is a coefficient of proportionality between Lagrangian and Eulerian integral timescales usually assumed to be between 1 and 2 (Shao, 2000), σ_w^2 is the vertical velocity variance, and $\phi_w(\zeta)$ is the MO similarity function for σ_w/u_*. The dependence of α_{tc} on ζ is not strong (see empirical fits for $\phi_w(\zeta)$ in Kaimal and Finnigan (1994)) and it complicates the obtention of a closed form solution to Equation (2). Therefore, in the present analysis, this dependence in neglected and the neutral stability value $\phi_w(\zeta)$=1.25 is used. Under these condition, integration of equation (2) yields

$$\frac{\overline{C}}{\overline{C}_r} = \left(\frac{\Phi}{\overline{C}_r w_s} + 1\right)\left(\frac{z}{z_r}\right)^{-\gamma} \exp(\gamma \psi_c) - \left(\frac{\Phi}{\overline{C}_r w_s}\right), \tag{12}$$

where $\gamma = w_s \alpha_{tc}/(\kappa u_*)$ and $\psi_c \equiv \int_{z_r/L}^{z/L} \frac{(1-\phi_c(x))}{x} dx$. The solution (12) is general and requires specification of $\phi_c(\zeta)$. If equations (7) are used, one obtains

$$\psi_c = \begin{cases} 2\ln\left(\frac{1+(1-16z/L)^{1/2}}{1+(1-16z_r/L)^{1/2}}\right), & \text{if } \zeta < 0, \\ -5z/L + 5z_r/L, & \text{if } \zeta > 0, \\ 0, & \text{if } \zeta = 0. \end{cases} \tag{13}$$

The final model for $\overline{C}/\overline{C}_r$ (Equation (12)) is now complete and it has the correct limits. When the trajectory-crossing effect in neglected ($\alpha_{tc} = 1$) and $\zeta \to 0$, it recovers Kind's model (Equation (4)), and when $w_s \to 0$ it recovers the MO similarity theory for a passive scalar, which is given by

$$\frac{\overline{C}}{\overline{C}_r} = 1 - \frac{\Phi}{\kappa u_* \overline{C}_r}\left[\ln\left(\frac{z}{z_r}\right) - \psi_c\left(\frac{z}{L}, \frac{z_r}{L}\right)\right]. \tag{14}$$

Figure 1 illustrates some examples of Equation (12) for particles with diameter $D_p = 10$ and $20\,\mu$m, for neutral, unstable ($L = -5$ m) and stable ($L = 5$ m) atmospheric stratifications over emitting ($\Phi > 0$) and depositing ($\Phi < 0$) surfaces. It is clear from the figure that both atmospheric stability and particle size have a strong effect on the shape of the mean concentration profiles.

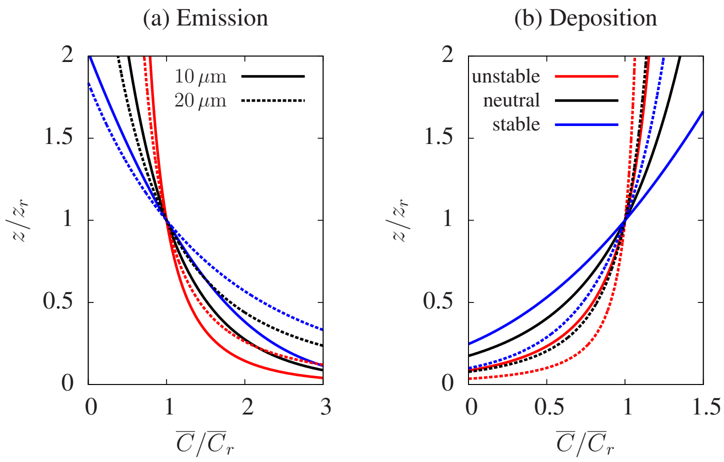

Fig. 1 Examples of profiles obtained from Equation (12) for particles with diameter $D_p = 10$ (solid lines) and $20\,\mu$m (dashed lines), with unstable ($L = -5$ m, red), neutral (black) and stable ($L = 5$ m, blue) ABLs. Arbitrary values of $u_* = 0.2\,\mathrm{m\,s^{-1}}$, $\Phi/C_r = 0.05\,\mathrm{m\,s^{-1}}$ (net emission) and $\Phi/C_r = -0.05\,\mathrm{m\,s^{-1}}$ (net deposition) were used.

The main differences between the proposed model and equation (8) presented by Chamecki et al. (2007) are the inclusion of the trajectory-crossing effects and the assumption that here only the turbulent flux is affected by atmospheric stability, while in equation (6) the settling flux is also modified by ζ. Although the changes introduced by buoyancy in the turbulence properties can potentially impact gravitational settling of inertial particles, in the present case the particle response time scale is so small that this effect is expected to be negligible.

3 Large-Eddy Simulation of dust concentration in the atmospheric boundary layer

The numerical simulations are designed to represent the evolution of dust profiles over an infinite and horizontally homogeneous dust source or sink. The LES code used in this study solves the three-dimensional filtered momentum equations in a rotating frame of reference, using a numerical discretization that combines a fully dealiased pseudo-spectral numerical method in the horizontal directions and a second order centered finite-differences method in the vertical direction. The fully explicit second-order Adams-Bashforth scheme is used for time integration. The scale-dependent Lagrangian averaged dynamic Smagorinsky model is used as sub-grid scale model, as described by (Bou-Zeid et al., 2005). The same LES implementation used here has been shown to produce mean velocity and temperature gradients in the atmospheric surface layer in agreement with MO similarity theory for both unstable and stable stratifications (Kleissl et al., 2006). More details about the code can be obtained from the detailed description in Kumar et al. (2006).

The simulations are designed to represent the atmospheric boundary layer (ABL) driven by a mean constant pressure gradient in geostrophic balance above the ABL. The horizontal boundary conditions are periodic. A stressfree boundary condition is applied at the top of the domain, which is located above the temperature inversion that represents the top of the ABL. Momentum fluxes at the bottom of the domain are calculated using Monin-Obukhov similarity theory as described in Kumar et al. (2006).

Dust particles are simulated using a concentration field as described by Chamecki et al. (2009). A filtered advection-diffusion equation including an additional term to represent gravitational settling (with constant settling velocity in the vertical direction) is used. The equation is discretized using a finite-volume approach and advection is represented by the flux-limiting scheme SMART (Gaskell and Lau, 1988) (see also Chamecki et al. (2008) for more details). The constant settling velocity w_s is defined by the terminal settling velocity in a still fluid and it is calculated via Stokes' law for a spherical particle

$$w_s = \frac{D_p^2 \rho_p g}{18\mu}, \tag{15}$$

where D_p and ρ_p are the diameter and density of the particle respectively, and μ is the dynamic viscosity of air.

A surface flux of dust Φ is imposed as a lower boundary condition over the entire horizontal domain. This flux represents the net flux at the surface, which should correspond to the imbalance between the emission and the deposition of particles. In the case of net emission of dust particles, a constant positive Φ was imposed. For the simulations representing a net deposition flux, Φ is obtained from the concentration in the first grid node, using Equation (4) (Kind's model), which can be justified by the assumption that the atmospheric stability effects very close to the surface are negligible. As can be observed from the results presented next, this assumption does not affect the influence of atmospheric stability on the mean concentration profile.

3.1 Summary of simulations

Two sets of simulations were performed. The first set, designed to study dust profiles above emitting dust sources, included neutral and unstable ABLs, for particles with $D_p = 1, 10, 20$ and $30\,\mu$m (with settling velocities $w_s = 7.98 \times 10^{-5}, 7.98 \times 10^{-3}, 3.19 \times 10^{-2}$ and $7.18 \times 10^{-2}\,\mathrm{m\,s^{-1}}$, respectively). The second set, designed to study dust deposition, included neutral, unstable and stable ABL for particles with $D_p = 1$ and $10\,\mu$m. Table 1 shows the physical domain and grid resolution of each stability case simulated. In all simulations, the domain was topped with a thermal inversion with a strength of $0.1\,\mathrm{K\,m^{-1}}$ (the strong inversion layer was intended to reduce the growth of the ABL in the convective simulations, allowing for appropriate statistical sampling under nearly steady-state conditions).

The main simulation parameters used for each case are presented in Table 2. Note that there is a small difference between the initial ($z_{i,0}$) and final ($z_{i,f}$) values of the ABL height (except for the stable case). The value of $-z_i/L \approx 30$ in the unstable simulations over a source is close to the lower limit of free convection, in order to evaluate how the models behave in this "extreme" situation. Because in this case in the surface layer $-z/L$ goes from 0 to approximately 3, the MO similarity theory is still expected to hold.

Table 1 Simulations setup: domain and grid size.

	domain ($x \times y \times z$, m)	# of grid points	grid size (m)
neutral	$3000 \times 3000 \times 1000$	$160 \times 160 \times 320$	$18.75 \times 18.75 \times 3.125$
unstable	$3000 \times 3000 \times 1000$	$160 \times 160 \times 320$	$18.75 \times 18.75 \times 3.125$
stable	$480 \times 480 \times 160$	$160 \times 160 \times 320$	$1.5 \times 1.5 \times 0.5$

Table 2 Simulation setup: physical parameters. $z_{i,0}$ and $z_{i,f}$ are the initial and final ABL heights respectively, (U_g, V_g) are the horizontal components of geostrophic wind, $\overline{w'\theta'}_0$ is the surface heat flux, u_* is the fiction velocity and L is the Obukhov length. Emission (emi.) and deposition (dep.) cases.

	$z_{i,0}$ (m)	(U_g, V_g) ($\mathrm{m\,s^{-1}}$)	$\overline{w'\theta'}_0$ ($\mathrm{K\,m\,s^{-1}}$)	u_* ($\mathrm{m\,s^{-1}}$)	L (m)	$z_{i,f}$ (m)	z_i/L
neutral (emi./dep.)	570	$(16, 0)$	0	0.40	$-\infty$	570	0
unstable (emi.)	570	$(10, 0)$	0.24	0.40	-20	600	-30
unstable (dep.)	570	$(10, 0)$	0.05	0.35	-62	590	-9.5
stable (dep.)	120	$(8, 0)$	-0.01	0.15	24	90	3.75

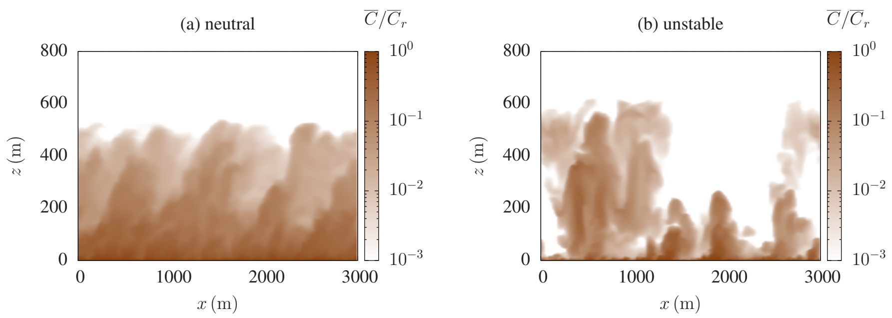

Fig. 2 Snapshots of normalized particle concentration field ($\overline{C}/\overline{C}_r$), for $D_p = 10\,\mu$m, for emission simulations in (a) neutral and (b) unstable ABL.

All simulations were first run without dust particles for a period corresponding to ~ 3 h in the neutral simulations and ~ 1 h in the unstable and stable simulations, for turbulence to spin up and reach steady-state conditions. Then the dust concentration was initialized with zeroes in the emission case and with a constant value of $\overline{C}(z)/\overline{C}_r = 1$ in the entire ABL for the deposition case. The surface of the domain was flat with a roughness $z_0 = 0.001$ m, and the surface flux of dust was set equal to $0.2\,\mu\mathrm{g\,m^{-2}\,s^{-1}}$ for all emission simulations. As an example, Fig. 2 shows snapshots of the particle concentration field in the emission case for neutral and unstable ABL, for particles $10\,\mu$m of diameter. The figure illustrates the differences in instantaneous concentration fields between the two cases (note the convective plumes generated in the unstable case, with large concentration in the updrafts and nearly clean downdrafts).

4 Results

4.1 The applicability of the steady-state assumption

An important assumption of the equilibrium models discussed here is that the mean concentration field is in steady state within the atmospheric surface layer (i.e., $\partial\overline{C}/\partial t$ can be neglected). If the unsteady term is not neglected, Equation (1) can be integrated in the vertical direction to yield (once again neglecting Brownian diffusion)

$$\overline{w'c'} - w_s\overline{C} = \Phi - \int_{z_0}^{z} \frac{\partial\overline{C}}{\partial t} dz. \tag{16}$$

In this equation, the left hand side corresponds to the total vertical dust flux. On the right hand side, Φ is the net surface flux and the second term must carry all the vertical and time dependence of the total flux. Over a source $\Phi > 0$ and we expect $\partial\overline{C}/\partial t > 0$, so that the unsteady term will be increasingly more negative as z increases. Thus, Equation (16) predicts that the total flux ($\overline{w'c'} - w_s\overline{C}$) should decrease with height (the opposite should happen in the case over a sink). All the solutions presented in Section 2 rely on the assumption that the unsteady term is negligible in comparison with the dominant terms in equation (16), and that the total flux is approximately constant within the surface layer (as is assumed to be the case for scalar fluxes in the Monin-Obukhov similarity framework).

Because the steady-state assumption is not invoked in the LES runs, simulation results can be used to assess its applicability. Figure 3 shows the time evolution of the ratio between the unsteady term of Equation (16) and the turbulent flux $\overline{w'c'}$ approximately in the middle of the surface layer (i.e., at $z = 0.05z_i$ – hereafter it is assumed that the surface layer extends up to $z = 0.1z_i$) for all simulations. In the figure, time is measured from the start of the dust initialization, and it is normalized by the eddy turnover time scale T_{eddy} for each simulation, which is given by $T_{\text{eddy}} = z_i/u_* \sim 1400\,\text{s}$ for neutral simulations, $T_{\text{eddy}} = z_i/w_* \sim 300\,\text{s}$ for unstable simulations (w_* is the convective velocity scale) and $T_{\text{eddy}} = z_i/u_* \sim 550\,\text{s}$ for stable simulations. In the beginning of the dust particle simulation, the unsteady term is dominant and the ratio is large due the spin-up time of the particle concentration field. After about one eddy turnover time, the ratio becomes approximately constant, at reasonably low values (typically smaller than 0.2 for neutral and stable simulations and much smaller than 0.1 for the unstable ones).

To provide further insight into the flux balance within the surface layer, Fig. 4 shows time-averaged vertical profiles of each term of Equation (16), for particles with $D_p = 1$ and $30\,\mu\text{m}$ for the emission case, and for particles with $D_p = 10\,\mu\text{m}$ for the deposition case. For emission of small particles ($D_p = 1\,\mu\text{m}$ in Fig. 4a), the settling flux $w_s\overline{C}$ (blue) is negligible, and the turbulent flux $\overline{w'c'}$ (red) is approximately equal to the surface net flux Φ (magenta). The small difference is balanced by the unsteady term (black), which becomes larger with increasing height. This is true for neutral (solid lines) and unstable (dashed lines) temperature stratifications. For emission of large particles ($D_p = 30\,\mu\text{m}$) in the neutral case (Fig. 4b, solid lines) the turbulent flux (red) is mainly balanced by the settling flux (blue), and the surface net flux Φ (magenta) is small compared to those fluxes (suggesting that Prandtl's solution is a good approximation for these larger particles). In the unstable case (Fig. 4b, dashed lines) turbulent flux (red) and

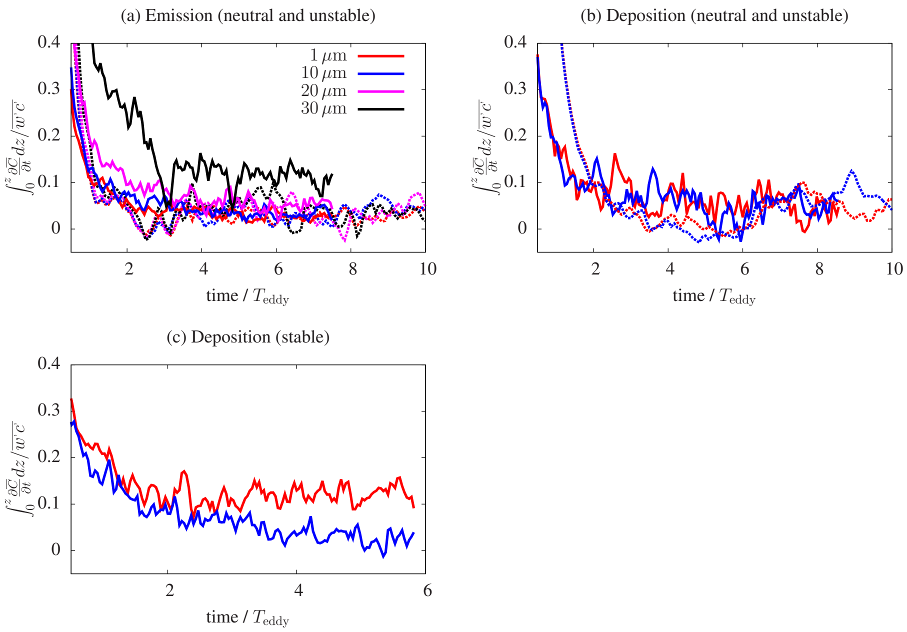

Fig. 3 Time evolution of the ratio between the unsteady term of Equation (16) and the turbulent flux, at $z/z_i \sim 0.05$, for all particle sizes. (a) Emission simulations, neutral ABL (solid lines) and unstable ABL (dashed lines). (b) Deposition simulations for neutral ABL (solid lines) and unstable ABL (dashed lines). (c) Deposition simulations for stable ABL. All times are normalized by the eddy turnover time scale for the ABL T_{eddy}.

gravitational settling (blue) are important, but so is their difference (i.e., the net flux is not negligible). In the deposition case (Fig. 4c) the turbulent flux (red) and gravitational settling (blue) are important and balanced by the surface net deposition flux (magenta) for all atmospheric stabilities, with minor contribution from the unsteady term.

In general, Fig. 4 suggests that in the surface layer ($z \lesssim 0.1z_i$), the unsteady term (black) is smaller than the other terms in Equation (16) for a range of particle sizes and atmospheric stabilities. Therefore, according to the present simulation results, the error incurred by neglecting the unsteady term (i.e. the equilibrium assumption) is acceptable. The worst case scenario is for a passive scalar ($w_s \to 0$) in neutral temperature stratification near the top of the surface layer, where the unsteady term reaches about 25% of the surface flux. The relative importance of the unsteady term always increases with height, becoming significant above the surface layer. Therefore, even though the total loading of particles is evolving in time, the surface layer profile evolves in an approximate self-similar form that may be represented by equilibrium models.

It is often assumed that, over a source, the equilibrium state is only reached when the net surface flux is equal to zero ($\Phi = 0$), a condition that may require very long time periods to be reached (e.g., Hoppel et al. 2002). As can be observed from the results presented here, this hypothesis is not needed for the establishment of an approximate steady-state condition. Furthermore, for very small particles the

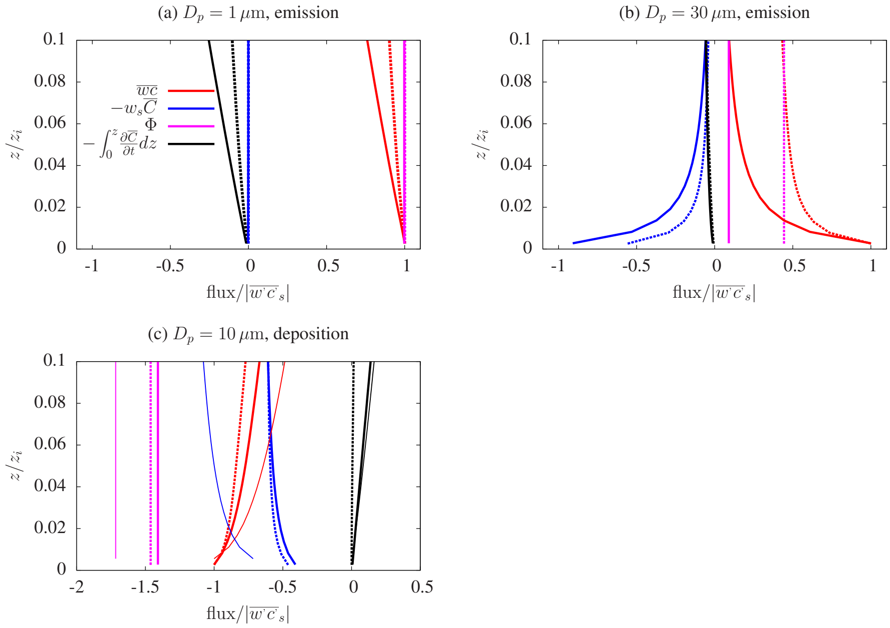

Fig. 4 Vertical profiles of each term of the unsteady flux equation (16) normalized by the absolute value of the turbulent flux at the surface ($|\overline{w'C'}_s|$), for particles with (a) $D_p = 1\,\mu$m and (b) $D_p = 30\,\mu$m for emission simulations under neutral (solid lines) and unstable (dashed lines) ABL, (c) $D_p = 10\,\mu$m for deposition simulations under neutral (solid lines), unstable (dashed lines) and stable (thin lines) ABL.

surface emission flux is in equilibrium with the turbulent flux, which corresponds to the MO similarity theory for scalars. Therefore, the only necessary conditions for the approximate validity of the steady-state assumption in the mean concentration (besides the constant surface flux) are the (1) statistical steady-state turbulence and (2) horizontally homogeneity of surface forcings. These are the same conditions required by MO similarity theory.

4.2 The estimation of mean vertical concentration profiles of dust

When comparing the theoretical equilibrium models (Equations (3), (4), (5), (8), (12) and (14)) with simulation results, the parameters needed in the models, such as u_*, L and Φ, were obtained from the corresponding simulation. In all the theoretical predictions, the trajectory-crossing effect has been neglected by setting $\alpha_{tc} = 1$. The lowest value of α_{tc} estimated from Equation (11) for the simulations presented here is $\alpha_{tc} \approx 0.99$, corresponding to the largest particle $D_p = 30\,\mu$m in the convective simulation with $u_* = 0.35\,\mathrm{m\,s^{-1}}$ (using the typical value $\beta = 1$). This is in agreement with Shao (2000), who concluded that for small dust particles the trajectory-crossing effect is only important in conditions with very weak turbulence. In addition, due to the different numerical approaches used for representing vertical advection in the momentum and particle concentration equations, a turbulent Schmidt number $Sc_t = 1.25$ is introduced in the theoretical profiles for comparisons with all simulations (this is equivalent to dividing $\phi_c(\zeta)$ by 1.25). This value corresponds to the ratio between eddy viscosity and particle eddy diffusivity for the simulations in the lower half of the surface layer ($z \lesssim 0.05\, z_i$), where Sc_t is approximately constant (this value is the appropriate Schmidt number for our simulations and it is not related to the trajectory-crossing effect, as it is independent of settling velocity). $\overline{C}_r$ is taken at the first vertical grid point ($z_r = 1.56\,\mathrm{m}$), and the results presented next are obtained by averaging the resolved concentration field in time and space (spatial averages are carried over the entire horizontal domain and time averages are carried over the last eddy turnover time of each simulation).

Figure 5 shows the normalized mean concentration profiles of dust in the neutral surface layer for the emission cases. It is clearly seen in the figure that, for the neutral surface layer, Kind's model (Equation (4)) is a good approximation for the entire range of particle sizes investigated (from 1 to 30 μm). The log-law model (Equation (5)) is indistinguishable from Kind's model for very small particles, here represented by $D_p = 1\,\mu\mathrm{m}$. Prandtl's power-law (Equation (3)) is a good approximation only for the largest particle size $D_p = 30\,\mu\mathrm{m}$. This suggests that for very large particles (which is the application intended by Prandtl, who was interested in profiles of blown snow and sand and sediment transport in rivers), the net flux is negligible when compared with settling and turbulent fluxes, as noted by Xiao and Taylor (2002) and clearly illustrated in Fig. 4b. For intermediate particle sizes particles ($D_p = 10\,\mu\mathrm{m}$ and $20\,\mu\mathrm{m}$), for which both w_s and Φ are important, only Kind's equation provides a good model to the mean concentration profiles. Note that the difference between the other models (log-law and power-law) and the simulation results for intermediate particle sizes increases with height.

Figure 6 is the unstable surface layer counterpart of Fig. 5. It is clearly seen in the figure that Kind's model (Equation (4)) is always far from the simulation results, showing the importance of atmospheric stability in determining the mean particle concentration profile for the conditions in the simulation ($u_* = 0.40\,\mathrm{m\,s^{-1}}$ and $L = -20\,\mathrm{m}$). Therefore, the most meaningful comparison is between the three models that include stability corrections: MO similarity for a passive scalar (14), the model proposed by Chamecki et al. (2007) (8), and the new model proposed here (12). The agreement between the model proposed here and the LES results is very good. The other models display poor performance for large particles ($D_p = 20$ and $30\,\mu\mathrm{m}$). As expected, the differences between the new model and the passive scalar behavior decrease as the particle size decrease, and the two are again indistinguishable for the smallest particle size ($D_p = 1\,\mu\mathrm{m}$). Note how the model proposed by Chamecki et al. (2007) moves towards the new model and the passive scalar as particle size decrease from $D_p = 30$ to 20 and to $10\,\mu\mathrm{m}$, but it diverges from them for $D_p = 1\,\mu\mathrm{m}$ (moving toward Kind's profile as discussed in Section 2).

Results obtained for the deposition simulations are presented in Fig. 7, for all atmospheric stabilities and for particles with $D_p = 1$ and $10\,\mu\mathrm{m}$. As observed before, for $D_p = 1\,\mu\mathrm{m}$ the proposed model (or Kind's model in the neutral case) is equivalent to MO similarity model, but the later is very far from the simulation for larger particles (especially in the stable case). Although the use of Kind's model in unstable and stable conditions is not ideal, the error is not as large as in the emission case.

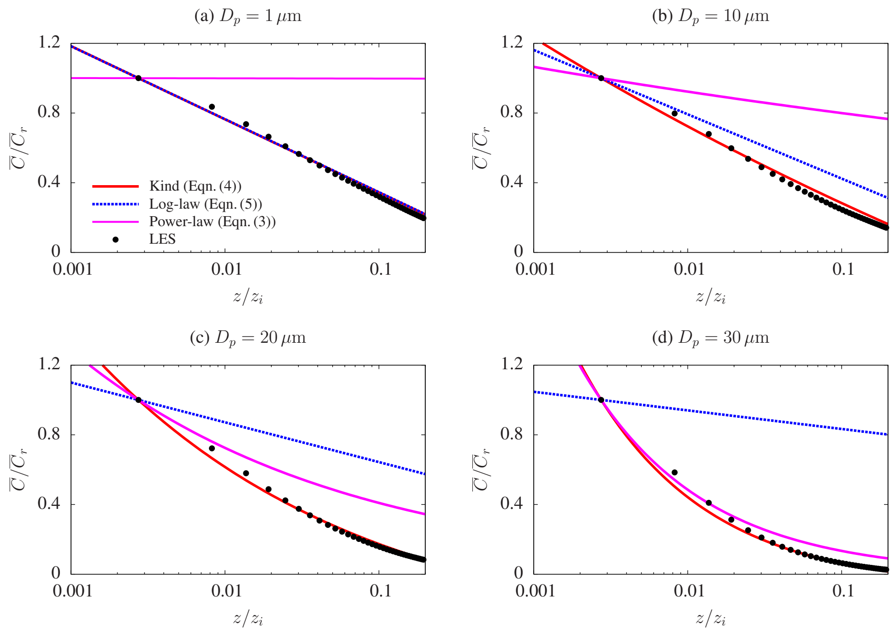

Fig. 5 Normalized mean vertical concentration profiles of dust in the neutral surface layer for different particle diameters (1, 10, 20 and 30 μm, as indicated in the figure).

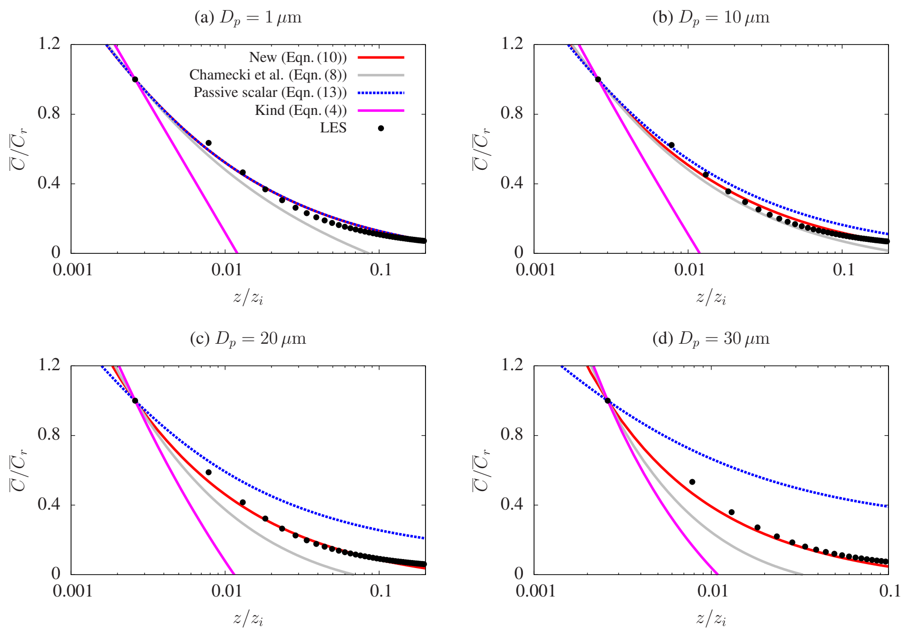

Fig. 6 Normalized mean vertical concentration profiles of dust in the unstable surface layer for different particle diameters (1, 10, 20 and 30 μm, as indicated in the figure).

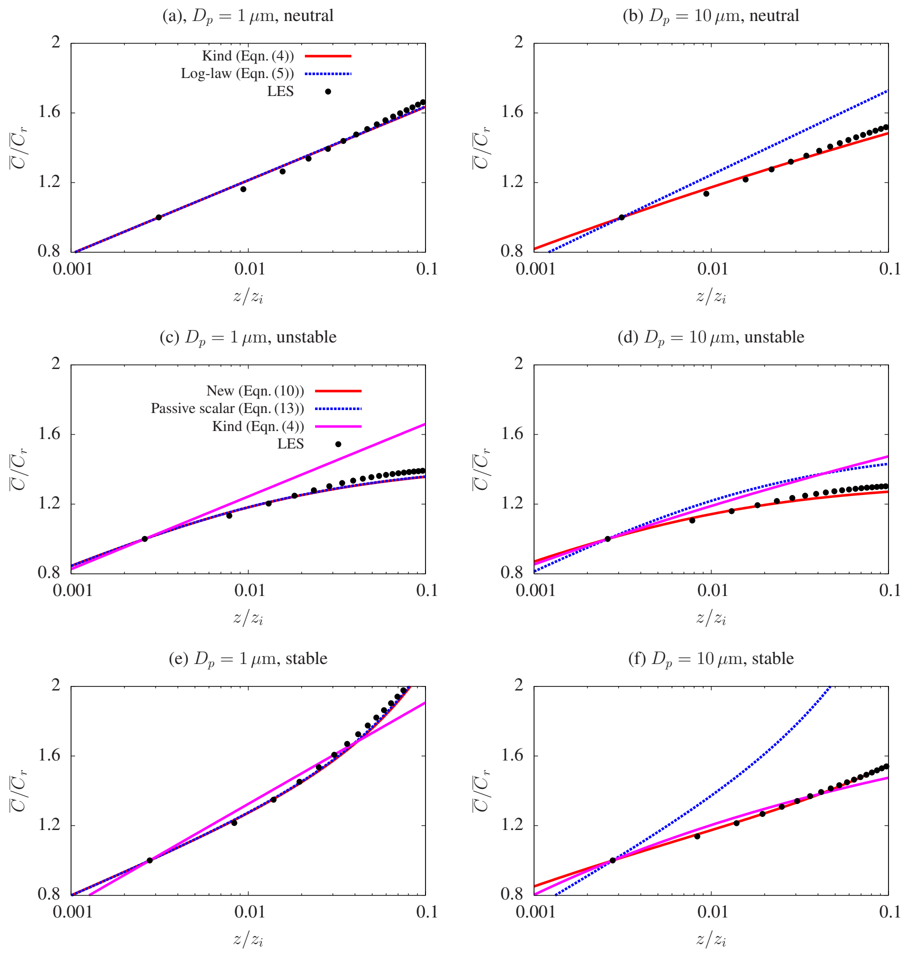

Fig. 7 Normalized mean vertical concentration profiles of dust in the deposition case for different particle diameters (1 and 10 μm) and atmospheric stability, as indicated in the figure.

Comparisons similar to the one presented in Fig. 6 were performed for other combinations of u_* and L ($u_* = 0.23$ and $0.34\,\mathrm{m\,s^{-1}}$, $L = -28$ and $-54\,\mathrm{m}$), yielding the same conclusion. These results show that the model proposed in Section 2.2 is capable of predicting the mean particle concentration profile for a wide range of stability and particle sizes, for emission and deposition cases.

As mentioned in previous subsection, after the first eddy turnover time the steady-state approximation is reasonable within the atmospheric surface layer. Because $\overline{C}_r$ evolves during the simulation, one approach to verify the validity of the equilibrium solution in time is to look at the simulation trajectory on the parameters space spanned by $\overline{C}/\overline{C}_r$ and $\Phi/\overline{C}_r w_s$. Trajectories from three heights within the surface layer are compared to those given by the equilibrium solution (12) in Fig. 8. For all simulations performed (only those for $D_p = 10\,\mu$m are

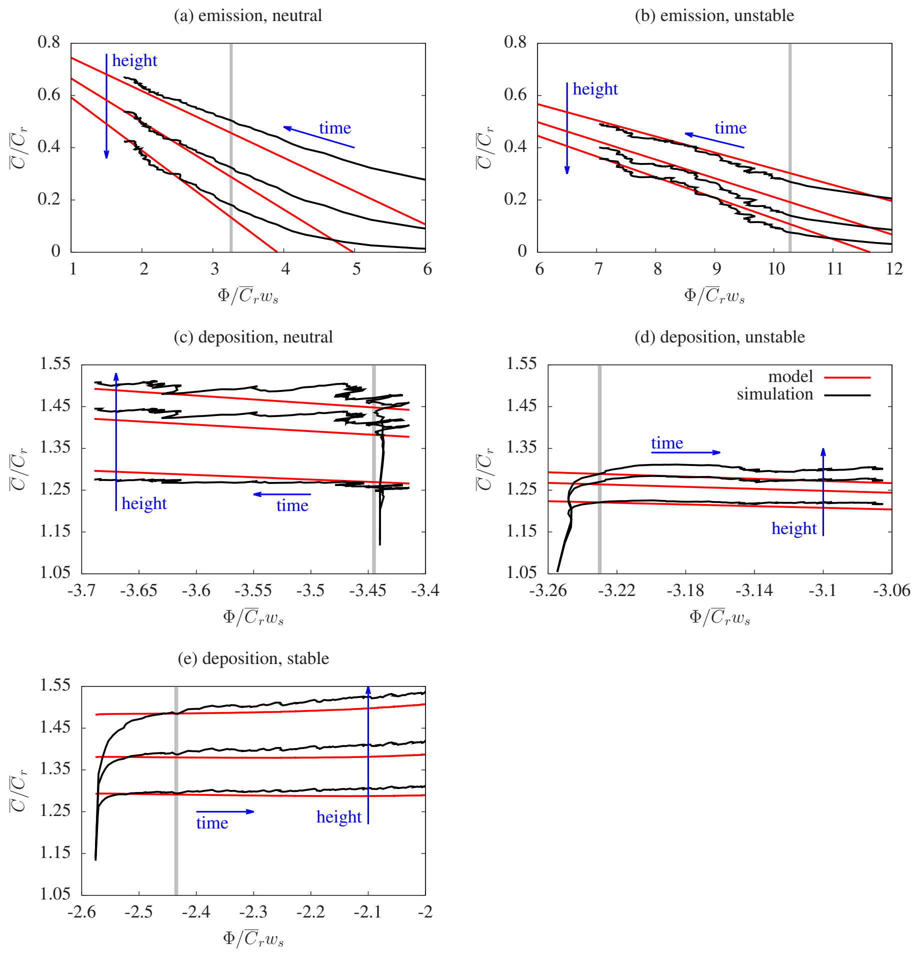

Fig. 8 Simulation trajectories on the parameters space spanned by $\overline{C}/\overline{C}_r$ and $\Phi/\overline{C}_r w_s$ (simulation time evolution, black line) for $D_p = 10, \mu$m at three different heights ($z = 0.02$, 0.05 and $0.09\, z_i$). The red line corresponds to the trajectory of the proposed equilibrium model (Equation 12). The vertical gray line identifies the time equal to one eddy turnover time ($t/T_{\rm eddy} = 1$).

shown), the trajectories approach the model during the initial stages (about one eddy turnover time) and then remain close to the predicted trajectory for the duration of the simulations, confirming the picture of a time evolving self-similar profile.

4.3 Surface flux estimations from concentration data

In this section we study the inverse problem: the estimation of the surface flux from mean concentration profiles. The goal is to assess the capabilities of the different equilibrium models in recovering the flux used to force the LES (i.e., the true surface flux in the simulation). In this analysis, mean concentration values at the first seven vertical grid points of the simulation are employed (this corresponds approximately to the lowest half of the surface layer; if additional points are used no significant differences are observed). Each model is fitted to the profile obtained from the simulations by estimating one single parameter: the value of the surface flux Φ. Figures 9a and c present the results for neutral simulations in the emission and deposition cases, respectively, where surface fluxes are normalized by $\overline{C}_r u_*$ (this makes all fluxes of the same order of magnitude). It is evident that Kind's model (Equation (4)) yields a very good estimate of the flux for all particle sizes. As expected from the results in the previous discussions, the log-law model produces accurate estimates for very small particles ($D_p = 1\,\mu$m), but it diverges quickly overestimating the magnitude of true flux when particles increase in size. It is worthwhile mentioning that both equations fit equally well to the simulated profile, but as illustrated in Fig. 9 yield very different estimates of the the surface flux.

The same analysis is performed for the unstable and stable atmospheric stratification cases, and the results are presented in Fig.s 9b, d and e. As expected from the previous section results, neglecting atmospheric stability and using Kind's model provides very poor estimates of the surface fluxes (underestimation for unstable with emission and stable with deposition, and overestimation for unstable with deposition). All the models that include stability corrections perform equally well for the smallest particle size, but only the newly proposed model yields good predictions of the surface flux across the range of particle sizes. Using MO similarity theory for passive scalars causes large over predictions of the fluxes, while the model proposed by Chamecki et al. (2007) produces under-prediction of the surface fluxes.

5 Conclusions

In this work a new equilibrium model relating surface flux and mean vertical profiles of dust concentration is proposed. The new model accounts for the effects of atmospheric stability (as characterized by $\zeta = z/L$) and particle settling velocity (w_s/u_*), and it recovers more specific models existent in the literature if the appropriate limits are used. It reduces to: (i) Kind's model (Chamberlain, 1967; Kind, 1992) for neutral stability, (ii) Prandtl's model (Prandtl, 1952) for neutral stability in the absence of a net flux of particles, (iii) the log-law (Monin, 1970) for neutral stability and no settling velocity, and (iv) MO similarity (Monin and Obukhov, 1954) for non-neutral stability and no settling velocity. In that sense, the resulting equation can be considered as an extension of Monin-Obukhov Similarity to concentration of settling particles.

Due to the difficulty in measuring surface fluxes of loose particles and the large variation in particle sizes during dust events, experimental validation of these models is difficult. The approach of fitting the value of the surface flux and comparing models by the mean squared errors of the adjusted equations (Gillies and Berkofsky, 2004; Chamecki et al., 2007) does not yield conclusive results. In this study we used numerical experiments based on LES of dust particles with four different sizes ($D_p = 1$, 10, 20 and 30 μm) in neutral and unstable atmospheric stabilities with emission and deposition situations to verify the applicability of the various models.

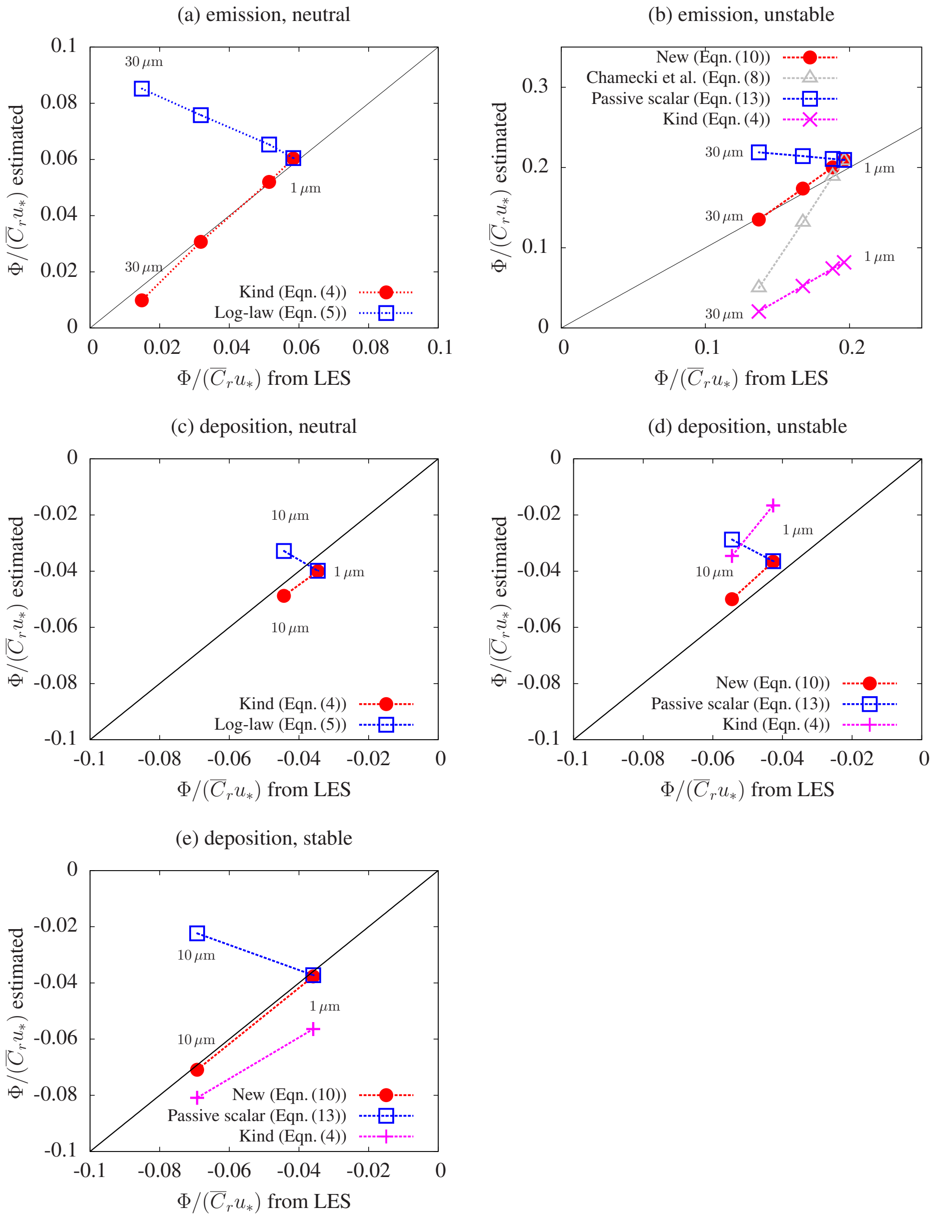

Fig. 9 Comparison between surface flux used to drive LES and the surface flux estimated by fitting theoretical profiles to mean concentration profile of the atmospheric surface layer. (a) Emission in neutral ABL, (b) emission in unstable ABL, (c) deposition in neutral ABL, (d) deposition in unstable ABL, and (d) deposition in stable ABL.

For the neutral atmospheric stability case, results presented here are the most convincing evidence to date that Kind's model is indeed the best approach to represent equilibrium profiles of suspended particles above extensive sources. The simulations also show that, in addition to the obvious limit towards the log-law as w_s/u_* becomes very small, the assumption of $\Phi = 0$ is indeed good when w_s/u_* is large (as already suggested by the one-dimensional simulations of Xiao and Taylor (2002)).

For unstable and stable atmospheric conditions the new model proposed here is in very good agreement with numerical simulations, performing much better than the model proposed by Chamecki et al. (2007). For the conditions used in the numerical simulations, effects of atmospheric stability on dust concentration profiles seem more important than gravitational settling. However, the picture would be different for lower values of the friction velocity. Therefore, we conclude that both effects are important and should be included in models that aspire to be applicable to realistic conditions.

Results also show that the steady-state assumption needed in the derivation of all the equilibrium models discussed here is reasonable for the atmospheric surface layer after the first eddy turnover time. Therefore, equilibrium models can be useful in the formulation of parameterizations for deposition fluxes typically needed in regional and global models.

Typically when the application requires estimating the surface flux from adjusting the concentration profiles to observations (Gillies and Berkofsky, 2004; Chamecki et al., 2007), different models present a similar performance measured by mean squared errors. However, the fitted values of the surface flux can be significantly different. This result is supported by the present study. In particular, the use of LES results where the surface flux is known clearly illustrates the poor predictions yielded by models that do not account for gravitational settling or atmospheric stability.

Acknowledgements LSF was funded by CNPq/Brazil through the program Science Without Borders. MC was supported by National Science Foundation grant AGS1358593.

References

Bou-Zeid E, Meneveau C, Parlange M (2005) A scale-dependent lagrangian dynamic model for large eddy simulation of complex turbulent flows. Phys Fluids 17(2):025105.

Chamberlain AC (1967) Transport of lycopodium spores and other small particles to rough surfaces. Proceedings of the Royal Society of London Series A Mathematical and Physical Sciences 296(1444):45–70.

Chamecki M, Meneveau C (2011) Particle boundary layer above and downstream of an area source: scaling, simulations, and pollen transport. J Fluid Mech 683:1–26.

Chamecki M, Hout R, Meneveau C, Parlange M (2007) Concentration profiles of particles settling in the neutral and stratified atmospheric boundary layer. Boundary-Layer Meteorol 125(1):25–38.

Chamecki M, Meneveau C, Parlange M (2008) A hybrid spectral/finite-volume algorithm for large-eddy simulation of scalars in the atmospheric boundary layer. Boundary-Layer Meteorol 128(3):473–484.

Chamecki M, Meneveau C, Parlange MB (2009) Large eddy simulation of pollen transport in the atmospheric boundary layer. J Aerosol Sci 40(3):241 – 255

Csanady GT (1963) Turbulent Diffusion of Heavy Particles in the Atmosphere. J Atmos Sci 20: 201–208.

Gaskell PH, Lau AKC (1988) Curvature-compensated convective transport: Smart, a new boundedness- preserving transport algorithm. Int J Numer Methods Fluids 8(6):617–641

Gillies J, Berkofsky L (2004) Eolian suspension above the saltation layer, the concentration profile. J Sediment Res 74(2):176–183.

Ginoux P, Chin M, Tegen I, Prospero JM, Holben B, Dubovik O, Lin SJ (2001) Sources and distributions of dust aerosols simulated with the GOCART model. J Geophys Res Atmos 106(D17):20,255–20,273.

Gong SL, Barrie LA, Blanchet JP, von Salzen K, Lohmann U, Lesins G, Spacek L, Zhang LM, Girard E, Lin H, Leaitch R, Leighton H, Chylek P, Huang P (2003) Canadian aerosol module: A size-segregated simulation of atmospheric aerosol processes for climate and air quality models 1. module development. J Geophys Res Atmos 108(D1):AAC 3–1–AAC 3–16.

Hoppel WA, Frick GM, Fitzgerald JW (2002) Surface source function for sea-salt aerosol and aerosol dry deposition to the ocean surface. J Geophys Res Atmos 107(D19):AAC 7–1–AAC 7–17.

Kaimal JC, Finnigan JJ (1994) Atmospheric boundary layer flows: their structure and measurement. Oxford University Press

Kind R (1992) One-dimensional aeolian suspension above beds of loose particles a new concentration-profile equation. Atmos Environ 26(5):927 – 931.

Kleissl J, Kumar V, Meneveau C, Parlange MB (2006) Numerical study of dynamic Smagorinsky models in large-eddy simulation of the atmospheric boundary layer: Validation in stable and unstable conditions. Water Resour Res 42(6):n/a–n/a.

Klose M, Shao Y (2013) Large-eddy simulation of turbulent dust emission. Aeolian Res 8(0):49 – 58.

Kok JF, Parteli EJR, Michaels TI, Karam DB (2012) The physics of wind-blown sand and dust. Rep Progr Phys 75(10):106,901.

Kumar V, Kleissl J, Meneveau C, Parlange MB (2006) Large-eddy simulation of a diurnal cycle of the atmospheric boundary layer: Atmospheric stability and scaling issues. Water Resour Res 42(6):n/a–n/a.

Lebedev, NN (1972) Special functions & their applications. Dover publications.

Monin A, Obukhov A (1954) Basic laws of turbulent mixing in the surface layer of the atmosphere. Tr Akad Nauk SSSR Geophiz Inst

Monin AS (1970) The atmospheric boundary layer. Annu Rev Fluid Mech 2(1):225–250.

Nho-Kim EY, Michou M, Peuch VH (2004) Parameterization of size-dependent particle dry deposition velocities for global modeling. Atmos Environ 38(13):1933 – 1942.

Pan Y, Chamecki M, Isard SA (2013) Dispersion of heavy particles emitted from area sources in the unstable atmospheric boundary layer. Boundary-Layer Meteorol 146(2):235–256.

Prandtl L (1952) Essentials of fluid dynamics. Blackie and Son, London

Shao Y (2000) Physics and Modelling of Wind Erosion. Kluwer Academic Publishers, Dordrecht

Tsoar H, Pye K (1987) Dust transport and the question of desert loess formation. Sedimentology 34(1):139–153.

Tsoar H, Pye K (1987) Dust transport and the question of desert loess formation. Sedimentology 34(1):139–153.

Xiao J, Taylor P (2002) On equilibrium profiles of suspended particles. Boundary-Layer Meteorol 105(3):471–482.

Zender CS, Bian H, Newman D (2003) Mineral dust entrainment and deposition (DEAD) model: Description and 1990s dust climatology. J Geophys Res Atmos 108(D14):n/a–n/a.

Zhao TL, Gong SL, Zhang XY, McKendry IG (2003) Modeled size-segregated wet and dry deposition budgets of soil dust aerosol during ace-asia 2001: Implications for trans-pacific transport. J Geophys Res Atmos 108(D23):n/a–n/a.